

# Shape-selective synthesis of CeO<sub>2</sub> via an EDTA-assisted route

Guozhu Chen · Sixiu Sun · Xinyu Song · Zhilei Yin ·  
Haiyun Yu · Chunhua Fan · Wei Zhao

Received: 18 July 2006 / Accepted: 10 November 2006 / Published online: 25 April 2007  
© Springer Science+Business Media, LLC 2007

**Abstract** Nanoparticles and sub-microrods of cubic CeO<sub>2</sub> were selectively prepared via an ethylenediamine tetraacetate (EDTA)-assisted route. They were characterized by transmission electron microscopy (TEM), X-ray powder diffraction (XRD), and infrared (IR) techniques. Controlling the reaction process, we obtained CeO<sub>2</sub> with different shapes. Sub-microrods were formed via an incomplete reaction while uniform nanoparticles were formed through a complete reaction between NaClO<sub>3</sub> and Ce–EDTA complexes. The addition of EDTA was critical to obtain CeO<sub>2</sub> sub-microrods and nanoparticles. Other experimental conditions, such as EDTA/Ce<sup>3+</sup> molar ratio and the reaction time were of importance in the final product morphology. A possible formation mechanism of CeO<sub>2</sub> was discussed.

## Introduction

Shape-selective synthesis of inorganic nanomaterials is of scientific and technological importance due to their unique

---

**Electronic supplementary material** The online version of this article (doi:10.1007/s10853-006-1254-6) contains supplementary material, which is available to authorized users.

---

G. Chen · S. Sun (✉) · X. Song · Z. Yin ·  
C. Fan · W. Zhao  
Department of Chemistry, Shandong University, Jinan,  
Shandong 250100, P.R. China  
e-mail: sxx@sdu.edu.cn

X. Song  
e-mail: songxy@sdu.edu.cn

H. Yu  
School of Materials Science and Engineering, Anhui University  
of Technology, Maanshan, Anhui 243002, P.R. China

shape-dependent properties and their promising application. Therefore, great efforts have been devoted to the synthesis of inorganic particles with various morphologies [1, 2]. Cerium (IV) oxide (CeO<sub>2</sub>) with a cubic fluorite-type structure, is an important material because its application is not only as an oxygen ion conductor in solid oxide fuel cells and oxygen monitors, but also as abrasive materials for chemical–mechanical planarization of advanced integrated circuits [3, 4]. Several techniques that include hydrothermal synthesis [5, 6], coprecipitation [7], flux method [8] and mechanical mixing [9] have been developed for the production of ceria. However, the reports on CeO<sub>2</sub> of different shapes selectively synthesized are scarce [5]. In particular, using the incomplete/complete reaction to control the shape is rarely reported [5–9].

M-EDTA is one of suitable precursors for the preparation of various materials under hydrothermal conditions. In addition, EDTA chelate precursors have been useful for controlling the crystal morphology under hydrothermal aging [10, 11].

In this paper, an EDTA-assisted method has been developed to selectively synthesize CeO<sub>2</sub> sub-microrods and nanoparticles, using Ce(NO<sub>3</sub>)<sub>3</sub> and NaClO<sub>3</sub> aqueous solutions as the reactants and EDTA as the modification agent. Furthermore, the shape-selective synthetic mechanism was investigated.

## Experimental section

All chemicals (Ce(NO<sub>3</sub>)<sub>3</sub> · 6H<sub>2</sub>O, Na<sub>2</sub>H<sub>2</sub>EDTA · 2H<sub>2</sub>O and NaClO<sub>3</sub>) were reagent grade and used without further purification. In a typical experiment, 0.217 g Ce(NO<sub>3</sub>)<sub>3</sub> · 6H<sub>2</sub>O was put into 5 mL of deionized water under stirring to form a homogeneous solution. Subsequently,

5 mL of 0.1 mol/L  $\text{Na}_2\text{H}_2\text{EDTA} \cdot 2\text{H}_2\text{O}$  aqueous solution was introduced into the above homogeneous solution under continuous stirring. After a few minutes, 2.5 mL of 0.5 mol/L  $\text{NaClO}_3$  aqueous solution was added into the above solution drop by drop under vigorous stirring. Then 12 mL slurry was transferred into a Teflon-lined stainless steel autoclave, sealed, and maintained at 180 °C for 8 h (sample 1) or 24 h (sample 2). After that, the autoclave was cooled down to room temperature naturally. The supernatant liquid was discarded and the remaining product was washed with deionized water and ethanol in sequence several times, and then separated by centrifugation. The product was dried in a vacuum oven at 60 °C for 12 h and then sample 1 was calcined with a muffle oven at 350 °C in air for 4 h (sample 3).

The samples were characterized by XRD on a Japan Rigaku D/Max- $\gamma$ A 200 X-ray diffractometer with  $\text{CuK}\alpha$  radiation ( $\lambda = 1.54178 \text{ \AA}$ ). TEM was carried out on a JEM-100CXII at an accelerating voltage of 100 kV. The samples for these measurements were dispersed in absolute ethanol by vibration in the ultrasonic pool. Then, the solutions were dropped onto a copper grid coated with amorphous carbon films and dried in air before measurement. Infrared spectra of the samples were obtained on a Nicolet T-IR5DX spectrometer.

## Results and discussion

The phase purity of the product was examined by the XRD pattern. Figure 1 shows the XRD patterns of the sub-microrods (sample 3) and nanoparticles (sample 2). All the peaks can be indexed to a face-centred cubic pure phase (space group:  $Fm\bar{3}m$  (225)) of ceria (JCPDS no. 81–0792). The morphology of the obtained product was shown in the TEM images (Fig. 2). The length of the sub-microrods was about 12  $\mu\text{m}$  and the diameter was about 250 nm. The size of the crystalline nanoparticles was about 40 nm, and all the resulting particles grew and developed into a good crystalline structure with polyhedral shape.

To understand the formation mechanism, the detailed growth process of  $\text{CeO}_2$  was carefully followed by time-dependent experiments. The effect of reaction time was investigated by fixing the temperature at 180 °C for 2, 6, 8, 12, 24 h, respectively. After heating for 2 h, the morphology of the product was microsheets as shown in the TEM images (Fig. 3a), but the product had poor crystallinity (inset in Fig. 3a). These microsheets should be a complex from the strong coordination interaction between cerium ions and EDTA. We believed that, before the hydrothermal reaction, the coordination occurred between EDTA and  $\text{Ce}^{3+}$  and formed complex, which was demonstrated by a change of the pH value. After EDTA solution

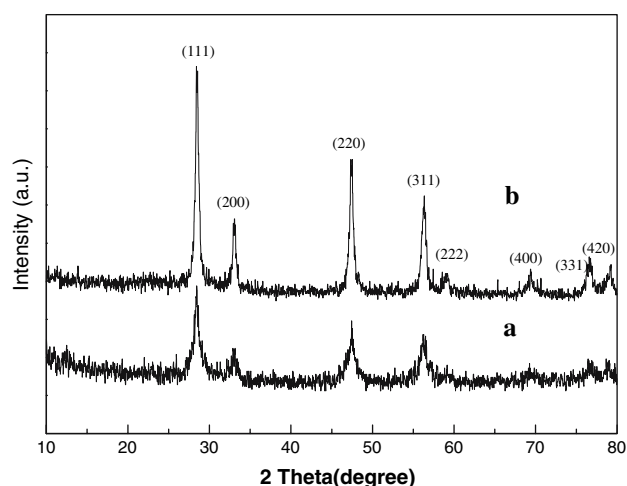


**Fig. 1** XRD patterns of the as-obtained samples: (a) sub-microrods and (b) nanoparticles

(pH  $\approx$  5) was added dropwise to  $\text{Ce}(\text{NO}_3)_3$  aqueous solution (pH  $\approx$  4.5) with stirring, the pH value of the resulting mixture was about 1.5. This phenomenon was attributed to the coordination reaction between EDTA and  $\text{Ce}^{3+}$ . In order to further investigate whether there was a coordination interaction between EDTA and cerium ions after hydrothermal 2 h, the FT-IR spectra were recorded as shown in Fig. 4. For well comparison, we also showed the IR spectra for  $\text{H}_4\text{EDTA}$ . The vibration frequencies of interest were the characteristic frequencies of the carboxyl group and the C–N anti-symmetrical and symmetrical stretching. The strongest and most characteristic absorption band for the carboxylate group ( $\text{COO}^-$ ) was in the 1,570–1,660  $\text{cm}^{-1}$  region and was due to the anti-symmetrical vibration of the  $\text{COO}^-$  group [12, 13]. The peak due to anti-symmetrical stretching vibration of  $\text{COO}^-$  group for Ce-EDTA occurred at the characteristic range 1596.65 (1,615–1,590  $\text{cm}^{-1}$ ) [12, 13] for metal–carboxyl bonding. It has been noted that the symmetrical and antisymmetrical C–N stretching bands in the Fig. 4b shift to longer wavelengths (smaller frequencies) compared with  $\text{H}_4\text{EDTA}$  (Fig. 4a). These results suggested that the cerium-nitrogen interaction occurred [14].

The evolution process of sub-microrods and nanoparticles from the microsheets at 180 °C was presented in Fig. 3. After 2 h, The XRD pattern of the microsheets indicated that  $\text{CeO}_2$  had not been produced but Ce–EDTA complexes appeared (See ESM, Fig. 1). When the hydrothermal reaction time was extended to 6 h, a mixture of the sheet-like particles and sub-microrods could be clearly observed from the TEM as shown in Fig. 3b. When the time was prolonged to 8 h, most sheet-like particles disappeared and sub-microrods with 250 nm in diameter and 12  $\mu\text{m}$  in length were formed (Fig. 3c). The diffraction of  $\text{CeO}_2$  was obviously strengthened by the XRD (See ESM,

**Fig. 2** TEM images of samples: (a) sub-microrods and (b) nanoparticles

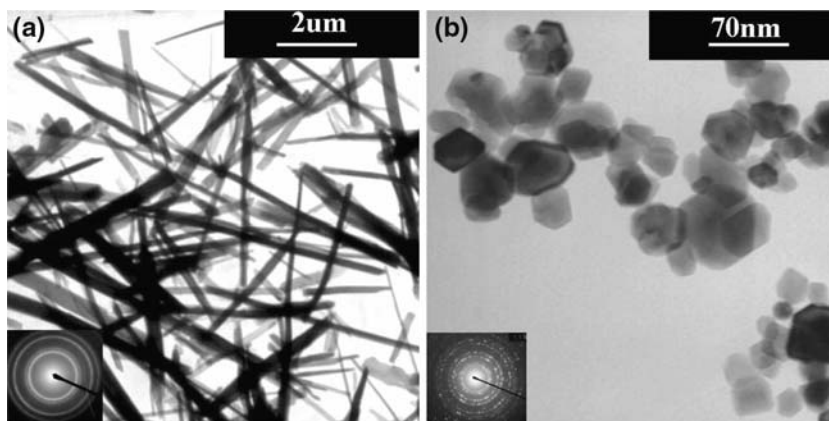
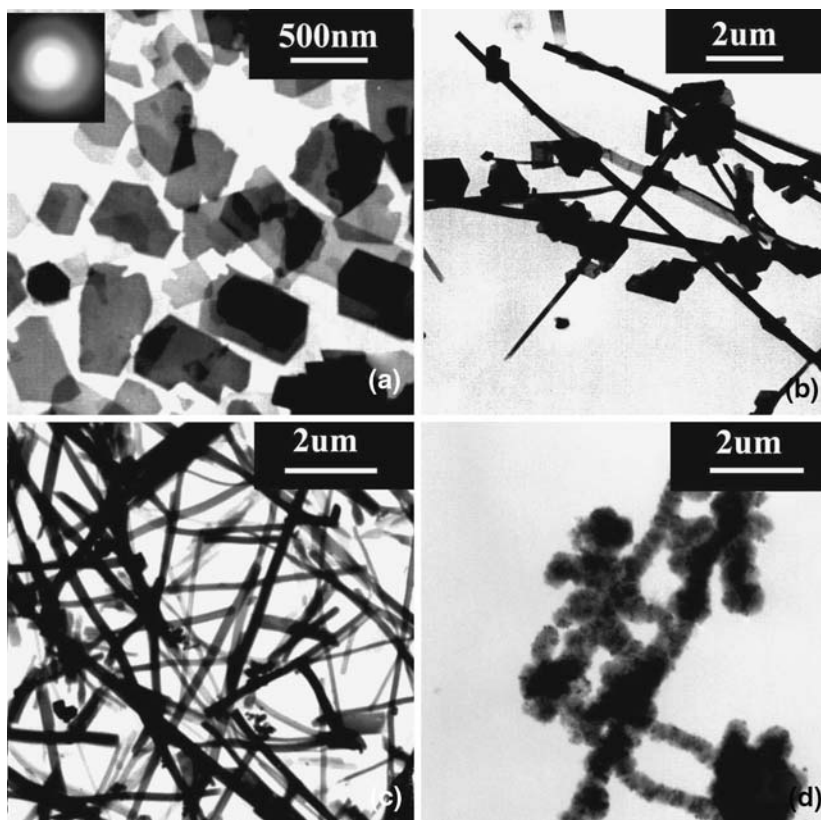


Fig. 1). In contrast, when the reaction time was prolonged to 12 h, rods consisting of nanoparticles were the predominant product (Fig. 3d). Furthermore, the sub-microrods had a tendency to break. After 24 h, the sub-microrods disappeared completely, and nanoparticles appeared (Fig. 2b). If the reaction time was fixed at 8 h, then the product was calcined with a muffle oven at 350 °C in air for 4 h with heating carefully, TEM images revealed that the sub-microrod shape of CeO<sub>2</sub> sustained after thermal treatment. The crystalline nature of the resultant CeO<sub>2</sub> sub-microrods and nanoparticles was verified by the selected

area electron diffraction (SAED) patterns (inset in Fig. 2), which were basically annular patterns. Like the XRD profile, the two annular patterns could be indexed to the fluorite crystal structure. It could be seen from the TEM images that the variation in the morphologies of the products with different reaction time was significant. The evolution process was similar to that of the needle-like barium sulfate using a barium-EDTA chelate precursor [15].

The presence of EDTA was crucial for the formation of CeO<sub>2</sub> sub-microrods and nanoparticles. Controlled experi-

**Fig. 3** Time-dependent growth progress illustrated by TEM images under hydrothermal conditions. (a) 2 h, (b) 6 h, (c) 8 h and (d) 12 h



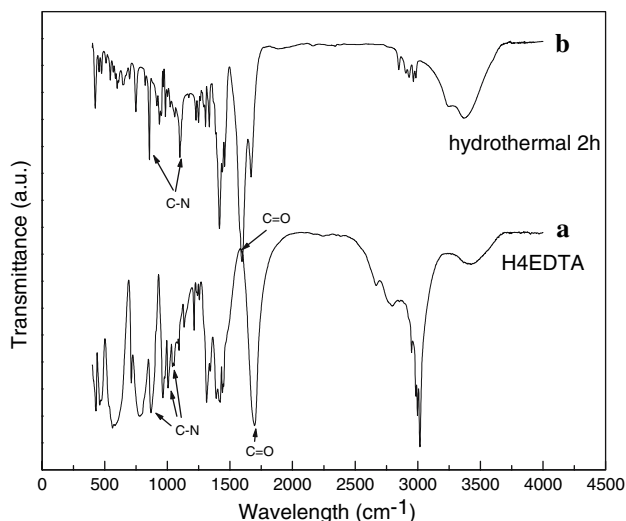
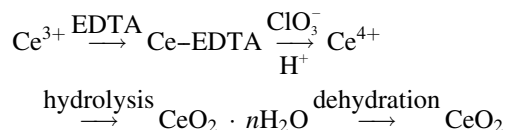


**Fig. 4** FT-IR spectra of the H<sub>4</sub>EDTA (a) and the sample in 180 °C hydrothermal reaction time 2 h (b)

ments have shown that only CeO<sub>2</sub> particles (average diameter ca. 2 μm) were obtained without EDTA (See ESM, Fig. 2A), and a sphere-like aggregation with an average width of 200 nm which consisted of many nanoparticles (See ESM, Fig. 2B) were formed at low concentration of EDTA. We concluded that, Ce–EDTA complex was unstable in the small [EDTA]/[Ce<sup>3+</sup>] molar ratio, thus, Ce<sup>3+</sup> ions were easily oxidized by the ClO<sub>3</sub><sup>-</sup>, which was similar to La–EDTA complexes [16]. In other way, the template effect decrease in the small [EDTA]/[Ce<sup>3+</sup>] molar ratio, so CeO<sub>2</sub> nanoparticles formed.

In fact, there are lone pair electrons on nitrogen and oxygen atoms in EDTA, which provide the possibility that the EDTA could combine with the Ce<sup>3+</sup> ions to form Ce–EDTA complexes. The complexes might serve as molecular templates in control of the crystals growth. The stability of the complexes results from the multiple sites within the ligand that gave rise to a cage-like structure, and is expected to decrease with the increase of the temperature. With the stability of the Ce–EDTA complexes decreased, the Ce<sup>3+</sup> ions dissociated slowly and the ClO<sub>3</sub><sup>-</sup> ions oxidized the Ce<sup>3+</sup> ions to the Ce<sup>4+</sup> under the acid condition that provided by the reaction between Ce<sup>3+</sup> and EDTA. As Ce<sup>4+</sup> ions were easily hydrolyzed, so the CeO<sub>2</sub> formed by the dehydration of CeO<sub>2</sub> · nH<sub>2</sub>O which was the hydrolysis result of Ce<sup>4+</sup>. Meanwhile, the mixture phases Ce–EDTA complexes and CeO<sub>2</sub> coexisted, which was confirmed by the XRD analysis (See ESM, Fig. 1). The chemical reactions course can be expressed concisely as follow:

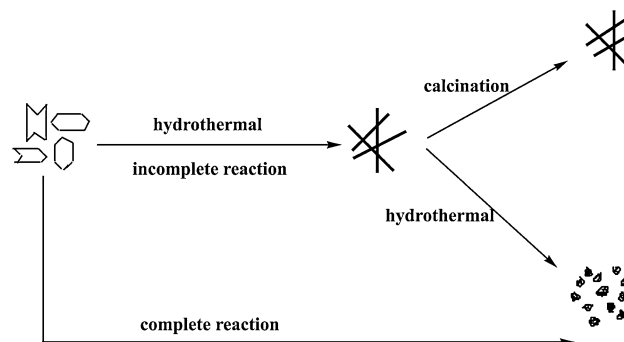


At appropriate reaction time, the uniform sub-microrods appeared with the mixture phases (Ce–EDTA and CeO<sub>2</sub>) (sample 1). It was noticed that this was an incomplete reaction, because excessive NaClO<sub>3</sub> would react with Ce–EDTA complexes continuously. When sample 1 calcined, the complexes phase disappeared and the CeO<sub>2</sub> phase remained, more importantly, the rod shape maintained after thermal treatment (sample 3). However, when extending hydrothermal time on the base of sample 1, the Ce–EDTA complexes dissociated unceasingly and the reaction went on, so the CeO<sub>2</sub> phase strengthened at the cost of the decrease of the complexes phase. Eventually, only CeO<sub>2</sub> phase existed.

The formation of sub-microrods and nanoparticles could be depicted as in Scheme 1.

## Conclusion

In summary, a simple EDTA-assisted hydrothermal process could be used for the selectively synthesizing of CeO<sub>2</sub>. Uniform sub-microrods and nanoparticles of cubic CeO<sub>2</sub> were selectively prepared by controlling the reaction process. Sub-microrods were formed by calcination and nanoparticles were formed by continuous reaction between the ClO<sub>3</sub><sup>-</sup> and complexes. In the process of the CeO<sub>2</sub> formation, EDTA acts not only chelating ligand but also template, which is an important role in forming the CeO<sub>2</sub>. Meanwhile, the reaction time, reaction temperature and the [Ce<sup>3+</sup>]/[EDTA] molar ratio were all influenced the morphology of CeO<sub>2</sub>. This one-pot solution approach offers an example for shape-selective synthesis based on incomplete/complete reaction, which also could be further extended as a facile route to access other inorganic materials with different shapes.



**Scheme 1** Schematic illustration of the possible formation process for sub-microrods and nanoparticles of CeO<sub>2</sub>

## References

1. Somiya S, Akiba T (1999) *J Eur Ceram Soc* 19:81
2. Ho C, Yu JC, Kwong T, Mak AC, Lai S (2005) *Chem Mater* 17:4514
3. Steele BCH (2000) *Solid State Ionics* 129:95
4. Feng XD, Sayle DC, Wang ZL, Paras MS, Santora B, Sutorik AC, Sayle TXT, Yang Y, Ding Y, Wang XD, Her YS (2006) *Science* 312:1504
5. Mai HX, Sun LD, Zhang YW, Si R, Feng W, Zhang HP, Liu HC, Yan CH (2005) *J Phys Chem B* 109:24380
6. Zhou K, Wang X, Sun XM, Peng Q, Li YD (2005) *J Catal* 229:206
7. Lee JS, Choi S-C (2004) *Mater Lett* 58:390
8. Chang HY, Chen HI (2005) *J Cryst Growth* 283:457
9. Li YX, Zhou XZ, Wang Y, You XZ (2003) *Mater Lett* 58:245
10. Fujishiro Y, Ito H, Sato T, Okuwaki A (1997) *J Alloys Compd* 252:103
11. Luo F, Jia CJ, Song W, You LP, Yan CH (2005) *Cryst Growth Des* 5:137
12. Shevchenko LL (1963) *Russ Chem Rev* 32:201
13. Sievers RE, Bailar JC Jr (1962) *Inorg Chem* 1:174
14. Flett MSC (1951) *J Chem Soc* 962
15. Uchida M, Sue A, Yoshioka T, Okuwaki A (2000) *J Mater Sci Lett* 19(15):1373
16. Fujishiro Y, Ito H, Sato T, Okuwaki A (1997) *J Alloys Compd* 252:103